

The Effect of Radiative Cooling on the Sunyaev-Zel'dovich Cluster Counts and Angular Power Spectrum: Analytic Treatment

Yu-Ying Zhang and Xiang-Ping Wu

National Astronomical Observatories, Chinese Academy of Sciences, Beijing 100012, China

ABSTRACT

Recently, the entropy excess detected in the central cores of groups and clusters has been successfully interpreted as being due to radiative cooling of the hot intragroup/intracluster gas. In such a scenario, the entropy floors S_{floor} in groups/clusters at any given redshift are completely determined by the conservation of energy. In combination with the equation of hydrostatic equilibrium and the universal density profile for dark matter, this allows us to derive the remaining gas distribution of groups and clusters after the cooled material is removed. Together with the Press-Schechter mass function we are able to evaluate effectively how radiative cooling can modify the predictions of SZ cluster counts and power spectrum. It appears that our analytic results are in good agreement with those found by hydrodynamical simulations. Namely, cooling leads to a moderate decrease of the predicted SZ cluster counts and power spectrum as compared with standard scenario. However, without taking into account energy feedback from star formation which may greatly suppress cooling efficiency, it is still premature to claim that this modification is significant for the cosmological applications of cluster SZ effect.

Subject headings: cosmology: theory — cosmic microwave background – galaxies: clusters: general — X-rays: galaxies

1. Introduction

With the rapid development of observing techniques (Birkinshaw, Hughes & Arnaud 1991; Jones et al. 1993; Birkinshaw & Hughes 1994; Carlstrom, Joy & Grego 1996; Myers et al. 1997; Hughes & Birkinshaw 1998; etc.), the Sunyaev-Zel'dovich (SZ) effect has become one of the most powerful tools for the detections of high redshift clusters (Joy et al. 2001) and cosmic microwave background (CMB) anisotropy on small scales (Mason et al. 2002). Indeed, the redshift-independence is the major advantage of non-targeted SZ surveys over

traditional optical and X-ray observations. This arises from the fact that the SZ effect depends uniquely on the intrinsic properties of the warm-hot gas associated with cosmic structures, whilst the photons interacting with the gas come from CMB at very high redshift $z \approx 1000$. Because robust constraints on cosmological models are provided by the most massive and distant clusters, growing interest over the past years has been focused upon how well the fundamental cosmological parameters can be constrained with non-targeted SZ cluster surveys (Molnar, Birkinshaw & Mushotzky 2002) and SZ power spectrum (Bond et al. 2002). The sensitivity of the expected SZ cluster counts and SZ power spectrum to the underlying cosmological model is quite impressive.

On arcminute scales, the strength of thermal SZ signals is directly proportional to the total thermal energy of the hot gas confined in clusters. Unlike the dark matter component of clusters whose dynamical behavior is governed purely by gravity, the intracluster gas is easily disturbed by many complicated physical processes in addition to gravity and thermal pressure, which include (non)gravitational heating, radiative cooling, star formation and energy feedback, magnetic fields, etc. The reliability of cosmological applications of SZ surveys on arcminute scales is closely connected with the question of how well one can handle these non-gravitational mechanisms. At present, a sophisticated treatment of the problem must rely on hydrodynamical simulations coupled with some semi-analytic approximations (e.g. da Silva et al. 2000, 2001; Seljak, Burwell & Pen 2001; Zhang, Pen & Wang 2002; White et al. 2002). Yet, the effective probe of cosmological models using non-targeted SZ surveys can be more easily achieved by semi-analytic approaches because of the requirement of the continuity in cosmological parameter space. It is thus desirable to understand the essential physics that dominates the dynamical evolution of intracluster gas.

While intracluster gas is mainly driven by gravitational shocks and adiabatic compression, two completely different mechanisms have been suggested thus far that may significantly affect the distribution of the intracluster gas: nongravitational preheating and radiative cooling. This is primarily motivated by the steepening of the X-ray luminosity-temperature relation and the entropy excess of groups and clusters reported by a number of investigators over the past years (e.g. David et al. 1993; Wu, Xue & Fang 1999; Ponman, Cannon & Navarro 1999). However, it has been realized that the prevailing preheating scenario is facing the so-called energy crisis – an unreasonably high efficiency of energy injection into the intracluster medium from supernovae must be required (Wu, Fabian & Nulsen 2000). Moreover, a uniform preheating of the cosmic baryons to a temperature of $\sim 10^6$ K would make the Ly α forest to disappear at high redshifts. In contrast, radiative cooling is a natural process of the hot intracluster gas, in which no exotic physics is needed. Several recent studies have shown that radiative cooling alone can allow one to successfully reproduce not only the observed distributions of global X-ray luminosity and entropy but also the internal structures of hot

gas in groups and clusters (Bryan 2000; Pearce et al. 2000; Muanwong et al. 2001, 2002; Voit & Bryan 2001; Wu & Xue 2002a,b; Borgani et al. 2002; Voit et al. 2002). If confirmed, this would have profound implications for our understanding of the evolution of hot gas and the formation of stars in the most massive systems in the universe.

So far, only can one employ hydrodynamical simulations to assess the effect of radiative cooling on the SZ counts and power spectrum (da Silva et al. 2000; White et al. 2002), while in the preheating scenario several (semi)analytic models have been applied for the prediction of SZ cluster surveys (Cavaliere & Menci 2001; Holder & Carlstrom 2001; Benson, Reichardt & Kamionkowski 2002). Now, a fully analytic treatment of radiative cooling effect on the prediction of SZ cluster counts and power spectrum may become possible if the observed central entropy floor of groups and clusters can be attributed to radiative cooling of hot intracluster/intragroup gas (Voit & Brayn 2001). In such a scenario, the minimum entropy of gas distribution in each cluster can be uniquely determined by the conservation of energy, which is equivalent to specifying the equation of state for the intracluster gas. Consequently, we will be able to derive the gas distribution of clusters at various redshifts as a result of cooling, in combination with the hydrostatic equilibrium hypothesis, provided that the underlying dark matter profile can be approximated by some kinds of analytic form, e.g., the universal density profile (Navarro, Frenk & White 1997; NFW). Together with the Press-Schechter (1994; PS) formalism for the abundance of dark halos at different cosmic epoch, we can eventually compare the predicted SZ counts and power spectra with and without radiative cooling, and demonstrate the uncertainty in the determination of the cosmological parameters arising from radiative cooling.

2. Gas distribution with and without cooling

2.1. Dark matter distribution

Intracluster gas with and without cooling is always assumed to be in hydrostatic equilibrium with the underlying gravitational potential dominated by dark matter component ρ_{DM} :

$$\frac{1}{\mu m_{\text{p}} n_{\text{e}}} \frac{d(n_{\text{e}} k_{\text{B}} T)}{dr} = - \frac{GM_{\text{DM}}(r)}{r^2}, \quad (1)$$

where n_{e} and T are the electron density and temperature, respectively, and $\mu = 0.585$ is the mean molecular weight. We use the universal density profile suggested by numerical simulations (NFW) for ρ_{DM}

$$\rho_{\text{DM}}(r) = \frac{\delta_{\text{c}} \rho_{\text{crit}}}{(r/r_{\text{s}})(1 + r/r_{\text{s}})^2}, \quad (2)$$

where δ_c and r_s are the characteristic density and length of the halo, respectively, and ρ_{crit} is the critical density of the universe at cosmic time t . We follow the prescription of Eke, Navarro & Steinmetz (2001) to fix the two free parameters, δ_c and r_s , in the NFW profile. To do this, the concentration parameter $c = r_{\text{vir}}/r_s$ of a dark halo identified at redshift z is related to the collapsing redshift z_{coll} through

$$c^3 = \frac{\Delta_c(z_{\text{coll}})}{\Delta_c(z)} \frac{\Omega_M(z)}{\Omega_M(z_{\text{coll}})} \left(\frac{1 + z_{\text{coll}}}{1 + z} \right)^3, \quad (3)$$

where Δ_c is the overdensity of dark halo within virial radius r_{vir} with respect to ρ_{crit} , for which we take $\Delta_c = 18\pi^2 + 82[\Omega_M(z) - 1] - 39[\Omega_M(z) - 1]^2$ for a flat universe, and $\Omega_M(z)$ is the cosmic density parameter. The collapsing redshift z_{coll} is determined by

$$D(z_{\text{coll}})\sigma_{\text{eff}}(M_s) = \frac{1}{C_\sigma}, \quad (4)$$

where D is the normalized linear growth factor, $C_\sigma = 25$ for Λ CDM model, and $\sigma_{\text{eff}}(M_s)$ is the so-called modulated rms linear density at mass scale M_s

$$\sigma_{\text{eff}}(M_s) = \sigma(M_s) \left[-\frac{d \ln \sigma(M_s)}{d \ln M_s} \right], \quad (5)$$

and M_s corresponds to the mass contained within $r = 2.17r_s$ where the circular velocity reaches the maximum. Finally, we specify a temperature T_{vir} to the hot gas in cluster of mass M at redshift z in terms of cosmic virial theorem (Bryan & Norman 1998)

$$k_B T_{\text{vir}} = 1.39 f_T (h^2 \Delta_c E^2)^{1/3} \text{ keV} \left(\frac{M}{10^{15} M_\odot} \right)^{2/3}, \quad (6)$$

in which we will choose the normalization factor to be $f_T = 0.92$, $E^2 = \Omega_M(1+z)^3 + \Omega_\Lambda + (1 - \Omega_M - \Omega_\Lambda)(1+z)^2$, and h is the Hubble constant in units of $100 \text{ km s}^{-1} \text{ Mpc}^{-1}$.

2.2. Gas distribution without cooling

In the absence of cooling, we adopt two models for the gas properties:

Model I – Gas is assumed to follow the same distribution as the dark matter in clusters:

$$n_e^0 = \frac{f_b}{\mu_e m_p} \rho_{\text{DM}} \quad (7)$$

in which f_b is the universal baryon fraction, and $\mu_e = 2/(1+X)$ is the mean electron weight with $X = 0.768$ being the hydrogen mass fraction in the primordial abundance of hydrogen

and helium. We solve the equation of hydrostatic equilibrium to get the temperature profile under the boundary restriction $T^0(r \rightarrow \infty) \rightarrow 0$:

$$k_{\text{B}}T^0(r) = k_{\text{B}}T^* \frac{r}{r_s} \left(1 + \frac{r}{r_s}\right)^2 \int_{r/r_s}^{\infty} \frac{(1+x) \ln(1+x) - x}{x^3(1+x)^3} dx, \quad (8)$$

where $k_{\text{B}}T^* = 4\pi G\mu m_p \delta_c \rho_{\text{crit}} r_s^2$.

Model II – Gas is assumed to be isothermal and $T^0(r) = T_{\text{vir}}$. In this case, the electron number density in terms of the equation of hydrostatic equilibrium reads (Makino, Sasaki & Suto 1998)

$$n_{\text{e}}^0(r) = n_{\text{e}0} e^{-\alpha} \left(1 + \frac{r}{r_s}\right)^{\alpha/(r/r_s)}, \quad (9)$$

where $\alpha = 4\pi G\mu m_p \delta_c \rho_{\text{crit}} r_s^2 / k_{\text{B}}T$. The normalization parameter $n_{\text{e}0}$ can be fixed through

$$\int_0^{r_{\text{vir}}} 4\pi \mu_{\text{e}} m_p r^2 n_{\text{e}}^0(r) dr = M_{\text{vir}} f_{\text{b}}. \quad (10)$$

2.3. Gas distribution with cooling

The cooling time scale for a steady, highly subsonic flow is determined by the conservation of energy. Setting the energy loss rate due to bremsstrahlung emission to equal the change in the specific energy of gas yields

$$t_{\text{c}} = 2.869 \times 10^{10} \text{yr} \left(\frac{1.2}{g(T^0)}\right) \left(\frac{k_{\text{B}}T^0}{\text{keV}}\right)^{1/2} \left(\frac{n_{\text{e}}^0}{10^{-3} \text{cm}^{-3}}\right)^{-1}, \quad (11)$$

where n_{e}^0 and T^0 are the electron number density and temperature without cooling, respectively, and g is the total Guant factor. If the cooling time t_{c} is chosen to be the age of clusters, or approximately the age of the universe, the above equation would allow us to set up a link between n_{e}^0 and T^0 . Note that this may lead to an overestimate of the cooling effect, and meanwhile t_{c} becomes to be cosmological model dependent. Perhaps, a more reasonable approach is to define the age of a cluster as the cosmic time between its collapsing redshift z_{coll} and the redshift z when it is identified (cf. Section 2.1). Once the gas density is specified, we will be able to work out the cooling radius and the amount of gas that cools out of the hot phase by the time t_{c} (e.g. Wu & Xue 2002b). The fate of the cooled materials within cooling radius may be associated with star formation. Now, our task is to work out the new distribution of the intracluster gas with cooling under different assumptions of the equation of state.

Model III – Before and after cooling, the equation of state for gas is always assumed to be isothermal and $T(r) = T_{\text{vir}}$. Consequently, the functional form of equation (9) also applies to the cooling case. However, the normalization after cooling is made through

$$\int_0^{r_{\text{vir}}} 4\pi\mu_e m_p r^2 n_e(r) dr = M_{\text{vir}} f_b - M_{\text{cool}} \quad (12)$$

where the total cooled material M_{cool} is given by

$$M_{\text{cool}} = \int_0^{r_{\text{cool}}} 4\pi\mu_e m_p n_e^0(r) r^2 dr, \quad (13)$$

$$= 4\pi f_b \delta_c \rho_{\text{crit}} r_s^3 \left[\ln \left(1 + \frac{r_{\text{cool}}}{r_s} \right) - \frac{r_{\text{cool}}}{r_s + r_{\text{cool}}} \right], \quad (14)$$

and r_{cool} is the cooling radius which can be obtained by combining equations (9) and (11).

Model IV – Gas traces dark matter (Model I) before cooling, and the equation of state for the new gas distribution after cooling is given by the entropy before cooling plus a constant entropy floor S_c (cf. Holder & Carlstrom 2001; Voit & Bryan 2001)

$$S = \frac{k_B T}{n_e^{2/3}} = S_c + \frac{k_B T^0}{(n_e^0)^{2/3}}, \quad (15)$$

where the entropy floor is determined by the cooling time t_c

$$\begin{aligned} S_c &= \frac{k_B T_{\text{vir}}}{(n_e^0)^{2/3}} \\ &= 100 \text{ keV cm}^2 \left(\frac{t_c}{2.869 \times 10^{10} \text{ yr}} \right)^{2/3} \left(\frac{g}{1.2} \right)^{2/3} \left(\frac{k_B T_{\text{vir}}}{\text{keV}} \right)^{2/3}. \end{aligned} \quad (16)$$

This “entropy floor” increases with cosmic time, resulting in a deposition of cooled materials in the central regions of clusters (Voit & Bryan 2001). Solving the equation of hydrostatic equilibrium yields

$$k_B T(r) = -\frac{2}{5} G \mu m_p S^{3/5}(r) \int_r^\infty \frac{M_{\text{DM}}(r)}{r^2} S^{-3/5}(r) dr, \quad (17)$$

and $n_e = (k_B T/S)^{3/2}$.

Model V – The same as Model IV except a varying metallicity $Z = 0.3Z_\odot(t/t_0)$ is assumed instead of $Z = 0.3Z_\odot$ for the rest four models, where t_0 denotes the present cosmic epoch. The parameters of the five models are summarized in Table 1.

3. Expectation for SZ cluster counts

The total SZ flux observed at frequency ν by a cluster of mass M at redshift z is (e.g. Barbosa et al. 1996)

$$S_\nu(x, M, z) = \frac{g_\nu(x)}{D_a^2(z)} \left(\frac{\sigma_T}{m_e c^2} \right) \int k_B T(r) n_e(r) 4\pi r^2 dr, \quad (18)$$

where

$$g_\nu(x) = 2 \frac{(k_B T_{\text{CMB}})^3}{(h_p c)^2} \frac{x^4 e^x}{(e^x - 1)^2} f_\nu(x); \quad (19)$$

$$f_\nu(x) = x \coth \frac{x}{2} - 4, \quad (20)$$

$x = h_p \nu / k_B T_{\text{CMB}}$, $T_{\text{CMB}} = 2.728$ K is the temperature of CMB (Fixsen et al. 1996), and D_a is the angular diameter distance to the cluster. In the isothermal case, the integral in the right hand of equation (18) can be replaced by the total mass of the cluster if the universal baryon fraction is introduced:

$$S_\nu = \frac{g_\nu(x)}{D_a^2(z)} \left(\frac{k_B T}{m_e c^2} \right) \left(\frac{f_b \sigma_T}{\mu_e m_p} \right) M. \quad (21)$$

This is the standard method adopted in the literature for the theoretical prediction of SZ cluster counts (Model II). While the assumption of isothermality is more or less reasonable in terms of current X-ray observations, the dependence of the gas fraction on temperature claimed by many observations throws doubt upon the direct utilization of equation (21). Nevertheless, if the gas fraction f_b is allowed to vary according to mass or temperature, or the total gas mass is replaced by the hot gas component alone, $M_{\text{gas}}(T)$, we may modify the above equation to be

$$S_\nu = \frac{g_\nu(x)}{D_a^2(z)} \left(\frac{k_B T}{m_e c^2} \right) \left(\frac{\sigma_T}{\mu_e m_p} \right) M_{\text{gas}}(T). \quad (22)$$

Table 1: The parameters and legend for the models of gas distribution.

Model	cooling	n_e	T	metallicity (Z_\odot)	line-style
I	no	gas-traces-mass	e.h.e.*	0.3	dot-dash
II	no	e.h.e.	isothermal	0.3	dashed
III	yes	e.h.e.	isothermal	0.3	dotted
IV	yes	gas-traces-mass	e.h.e.	0.3	solid
V	yes	gas-traces-mass	e.h.e.	$0.3(t/t_0)$	dash dot dot dot

*Obtained by solving the equation of hydrostatic equilibrium.

As shown in the above section, $M_{\text{gas}}(T)$ can be analytically determined for any cluster within the framework of radiative cooling. This provides a simple approach to estimating the effect of radiative cooling on SZ cluster counts without knowing the density distribution of the hot, isothermal gas inside clusters, which will be applied to Model III. For rest three models, I, IV and V, we will adopt the exact formula of S_ν , equation (18), in the theoretical prediction of SZ cluster counts.

The expected number of SZ selected clusters with flux greater than S_ν and in redshift interval $(z, z + dz)$ is

$$\frac{dN(> S_\nu)}{dzd\Omega} = \frac{dV}{dzd\Omega} \int_{M_{\min}(z, S_\nu)}^{\infty} \frac{dn}{dM} dM, \quad (23)$$

where the mass threshold $M_{\min}(z, S_\nu)$ is given by the definition of equation (18) or (21) or (22), depending on what approximation we would use. We adopt the PS mass function to describe the distribution of clusters

$$dn = -\sqrt{\frac{2}{\pi}} \frac{\bar{\rho}}{M} \frac{\delta_c(z)}{\sigma^2} \frac{d\sigma}{dM} \exp\left(-\frac{\delta_c^2(z)}{2\sigma^2}\right) dM, \quad (24)$$

where $\bar{\rho}$ is the mean cosmic density, δ_c is the linear over-density of perturbations that collapsed and virialized at redshift z , and σ is the linear theory variance of the mass density fluctuation in sphere of mass M :

$$\sigma^2(M) = \frac{1}{2\pi^2} \int_0^{\infty} k^2 P(k) |W(kR)|^2 dk, \quad (25)$$

and $W(kR) = 3(\sin x - x \cos x)/x^3$ is the Fourier representation of the window function. The power spectrum, $P(k) \propto k^n T^2(k)$, is normalized by the rms fluctuation on an $8 h^{-1}$ Mpc scale, σ_8 , and we take the transfer function $T(k)$ from an adiabatic CDM model given by Bardeen et al. (1986) for the Harrison-Zel'dovich case $n=1$. Note that our results may be moderately changed if a modified mass function of dark halos is adopted (e.g. Jenkins et al. 2001; Sheth & Tormen 2001).

We work with a flat cosmological model (Λ CDM) of $\Omega_b h^2 = 0.019$, $\Omega_M = 0.3$ and $\Omega_\Lambda = 0.7$. We adopt $\sigma_8 = 0.90$ and a Hubble constant of $h = 0.65$. We choose the SZ flux limit to be $S_\nu = 15$ mJy at frequency $\nu = 30$ GHz. We perform numerical calculations for the five models of gas distribution with and without cooling, and demonstrate the resulting differential SZ cluster counts in Figure 1. While there are some differences between the redshift distribution of clusters predicted by the gas-traces-mass assumption and the one by the isothermal assumption, the effect of radiative cooling leads to a moderate decrease in the expected number of SZ clusters although the peak locations with and without cooling remain

roughly the same. Alternatively, our prediction alters only slightly if the cosmic evolution of metallicity according to $0.3Z_{\odot}(t/t_0)$ is included.

Recall that in the standard treatment, the expectation for SZ cluster counts is made by presumably taking the intracluster gas to be isothermal and without cooling. If this prediction is directly applied to the determination of cosmological parameters in future SZ surveys, large uncertainty may be introduced because of the ignorance of radiative cooling correction. Now we can evaluate the uncertainty in the determination of cosmological parameters by comparing the theoretical predictions with and without radiative cooling. To do this, we still work with a flat cosmological model of $\Omega_M + \Omega_{\Lambda} = 1$, but allow Ω_M to vary according to σ_8 until the predicted redshift distribution of SZ cluster counts by the standard model (II) matches those by the cooling models III–V.

Figure 2 shows the resulting σ_8 versus Ω_M , in which the contours indicate 68% joint confidence intervals on the two parameters, corresponding to $\Delta\chi^2 = 2.30$. Uncertainties in Ω_M and σ_8 due to radiative cooling correction can be easily demonstrated by noticing that the true input values in the cooling models are $\Omega_M = 0.30$ and $\sigma_8 = 0.90$, while our best-fit results are $(\Omega_M, \sigma_8) = (0.24_{-0.11}^{+0.13}, 0.89_{-0.10}^{+0.08})$, $(0.23_{-0.11}^{+0.11}, 0.88_{-0.10}^{+0.08})$ and $(0.23_{-0.11}^{+0.10}, 0.89_{-0.10}^{+0.07})$ for the three cooling models III, IV, and V, respectively. Namely, without the correction of radiative cooling we might underestimate both Ω_M and σ_8 parameters for Λ CDM cosmological model, although within the uncertainties of our ‘observations’, the best-fit parameters are still consistent with the input values.

4. SZ Power spectrum

The angular power spectrum of temperature fluctuation on the CMB sky due to the SZ effect of clusters can be separated into the Poisson term $C_l^{(P)}$ and clustering term $C_l^{(C)}$ (Cole & Kaiser 1988; Komatsu & Kitayama 1999):

$$C_l^{(P)} = f_{\nu}^2(x) \int_0^{z_{\text{dec}}} dz \frac{dV}{dz} \quad (26)$$

$$\int_{M_{\text{min}}}^{\infty} dM \frac{dn(M, z)}{dM} |y_l(M, z)|^2, \quad (27)$$

and

$$C_l^{(C)} = f_{\nu}^2(x) \int_0^{z_{\text{dec}}} dz \frac{dV}{dz} P(k = l/D_0, z) \left[\int_{M_{\text{min}}}^{\infty} dM \frac{dn(M, z)}{dM} b(M, z) y_l(M, z) \right]^2, \quad (28)$$

where $z_{\text{dec}} \approx 1000$ is the CMB photon decoupling redshift, D_0 is the comoving distance to cluster of mass M at z , $y_l(M, z)$ is the Fourier transform of the Compton y -parameter in the thermal SZ effect: $\Delta T/T_{\text{CMB}} = f_\nu(x)y(\theta)$, $f_\nu(x)$ reflects the spectral dependence, and $b(M, z)$ is the so-called bias parameter, for which we use the analytic approximation of Mo & White (1996). In our numerical computation, the minimum cluster mass is taken to be $M_{\text{min}} = 1 \times 10^{13} M_\odot$, and our final results are unaffected by this choice if we focus on large-scale ($>$ arcminute) fluctuations on the CMB sky.

We illustrate in Figure 3 the SZ power spectra with and without cooling for the five models in Table 1, together with the primary CMB signal produced by CMBFAST. It appears that the power spectra predicted by the gas-traces-mass and isothermal assumptions become indistinguishable, and the total SZ power spectrum is dominated by the Poisson distribution of groups and clusters. Inclusion of radiative cooling leads to a significant decrease of SZ power spectrum, especially at small angular scales or high- ℓ . This is simply because cooling removes more efficiently the hot gas at the central regions of clusters and in low-mass groups, and therefore suppresses the SZ signal at small scales. This result is in good agreement with the one found by hydrodynamical simulations (e.g. da Silva et al. 2001).

5. Discussion and conclusions

As a natural process, radiative cooling plays an important role in the formation of galaxies. In the central regions of clusters and groups, the typical cooling time scale of the hot gas is usually less than the age of the universe. It follows that a considerable amount of the intracluster/intragroup gas must have cooled out of the hot phase since the formation of clusters and groups unless the cooling efficiency can be suppressed by other non-gravitational heating processes such as energy feedback from supernovae and AGN activity. Since cooling removes the hot gas in groups and clusters, it meanwhile reduces the SZ signal, leading to a decrease of the expected SZ cluster counts and power spectrum. This scenario has been confirmed by numerical simulations (e.g. da Silva et al. 2001) and our calculations based on a simple analytical model. If the excess entropy detected in the central cores of groups and clusters can be attributed to radiative cooling (Voit & Bryan 2001), some conclusions drawn from a phenomenological preheating model based on the observed entropy distribution can be equally applied to the cooling scenario. Indeed, it has been shown that the preheating model also results in a decrease of SZ cluster counts and power spectrum (e.g. Komatsu & Kitayama 1999; Holder & Carlstrom 2001; da Silva et al. 2001). Recall that current X-ray observations alone are still unable to distinguish between preheating and cooling models (e.g. Voit et al. 2002; Borgani et al. 2002).

It is well known that radiative cooling is a runaway process. Consequently, the expected cooled materials within the framework of radiative cooling from both hydrodynamical simulations and analytical approaches exceed the observed stellar mass fraction in the local universe (Balogh et al. 2001; Wu & Xue 2002b and references therein). Inclusion of star formation and energy feedback, which should in principle resolve the so-called cosmic cooling crisis, may significantly reduce the effect of radiative cooling on the X-ray properties and SZ signal of clusters. Indeed, recent numerical simulations by White et al. (2002) have shown that as a consequence of the combined effect of energy injection by star formation and radiative cooling, the SZ power spectrum remains roughly unchanged.

Our simple analytic approach to estimating the effect of radiative cooling on the non-targeted SZ cluster survey and SZ power spectrum yields a result consistent with those found by hydrodynamical simulations (e.g. da Silva et al. 2001). This analytic method allows an effective evaluation of the significance of various factors in the gas cooling process. For example, we have shown that within the framework of radiative cooling, both SZ cluster counts and power spectrum are insensitive to temperature variation. In other words, the isothermality hypothesis is a good approximation in the theoretical study of cluster SZ effect. Also, one may choose to use the gas-traces-mass assumption, which provides a reasonable description of the gas distribution outside the X-ray core. Recall that unlike the X-ray emission which depends on n_e^2 , the SZ signal is proportional to n_e . So, the gas outside the X-ray core makes an important contribution to SZ signal too. Finally, in order to eliminate the cooling crisis in the present model and include another natural process, i.e., heating by supernovae, in the evolution of hot gas, it is worth exploring how energy injection into the intracluster/intrgroup gas from star formation is incorporated into cooling scenario in a simple analytic way.

This work was supported by the National Science Foundation of China, and the Ministry of Science and Technology of China, under Grant No. NKBRSF G19990754.

REFERENCES

- Balogh, M. L., Pearce, F. R., Bower, R. G., & Kay, S. T. 2001, MNRAS, 326, 1228
- Barbosa, D., Bartlett, J. G., Blanchard, A., & Oukbir, J. 1996, A&A, 314, 13
- Bardeen, J. M., Bond, J. R., Kaiser, N., & Szalay, A. S. 1986, ApJ, 304, 15
- Benson, A. J., Reichardt, C., & Kamionkowski, M. 2002 MNRAS, 331, 71
- Birkinshaw, M., Hughes, J. P., & Arnaud, K. A. 1991, ApJ, 379, 466
- Birkinshaw, M., & Hughes, J. P. 1994, ApJ, 420, 33
- Bond, J. R., et al. 2002, ApJ, in press (astro-ph/0205386)
- Borgani, S., et al. 2002, MNRAS, in press (astro-ph/0205471)
- Bryan, G. L. 2000, ApJ, 544, L1
- Bryan, G. L., & Norman, M. L. 1998, ApJ, 495, 80
- Carlstrom, J. E., Joy, M., & Grego, L. 1996, ApJ, 456, L75
- Cavaliere, A., & Menci, N. 2001, MNRAS, 327, 488
- Cole, S. & Kaiser, N. 1988, MNRAS, 233, 637
- da Silva, A. C., Barbosa, D., Liddle, A. R., & Thomas, P. A. 2000, MNRAS, 317, 37
- da Silva, A. C., et al. 2001, ApJ, 561, 15
- David, L. P., et al. 1993, ApJ, 412, 479
- Dawson, K. S., et al. 2001, ApJ, 553, L1
- Eke, V. R., Navarro, J. F., & Steinmetz, M. 2001, ApJ, 554, 114
- Fixsen, D. J., et al. 1996, ApJ, 473, 576
- Holder, G. P., & Carlstrom, J. E. 2001, ApJ, 558, 515
- Hughes, J. P., & Birkinshaw, M. 1998, ApJ, 501, 1
- Jenkins, A., et al. 2001, MNRAS, 321, 372
- Jones, M., et al. 1993, Nature, 365, 320
- Joy, M., et al. 2001, ApJ, 551, 1
- Komatsu, E., & Kitayama, T. 1999, ApJ, 526, 1
- Makino, N., Sasaki, S., & Suto, Y. 1998, ApJ, 497, 555
- Mason, B. S., et al. 2002, ApJ, in press (astro-ph/0205384)
- Mather, J. C., Shafer, R. A., & Wright, E. L. 1996, ApJ, 473, 576

- Molnar, S. M., Birkinshaw, M., & Mushotzky, R. F. 2002, *ApJ*, 570, 1
- Mo, H.-J., & White, S. D. M. 1996, *MNRAS*, 282, 347
- Muanwong, O., Thomas, P. A., Kay, S. T., & Pearce, F. R. 2002, *MNRAS*, in press (astro-ph/0205137)
- Muanwong, O., Thomas, P. A., Kay, S. T., Pearce, F. R., & Couchman, H. M. P. 2001, *ApJ*, 552, L27
- Myers, S. T., Baker, J. E., Readhead, A. C. S., Leitch, E. M., & Herbig, T. 1997, *ApJ*, 485, 1
- Navarro, J. F., Frenk, C. S., & White, S. D. M. 1997, *ApJ*, 490, 493
- Pearce, F. R., Thomas, P. A., Couchman, H. M. P., & Edge, A. C. 2000, *MNRAS*, 317, 1029
- Ponman, T. J., Cannon, D. B., & Navarro, J. F. 1999, *Nature*, 397, 135
- Press, W. H., & Schechter, P. 1974, *ApJ*, 187, 425
- Seljak, U., Burwell, J., & Pen, U.-L. 2001, *Phys. Rev. D*, 63, 063001
- Sheth, R. K., Mo, H. J., & Tormen, G. 2001, *MNRAS*, 323, 1
- Voit, G. M., & Bryan, G. L. 2001, *Nature*, 414, 425
- Voit, G. M., Bryan, G. L., Balogh, M. L., & Bower, R. G. 2002, *ApJ*, in press (astro-ph/0205240)
- White, M., Hernquist, L., & Springel, V. 2002, *ApJ*, in press (astro-ph/0205437)
- Wu, K. K. S., Fabian, A. C., & Nulsen, P. E. J. 2000, *MNRAS*, 318, 889
- Wu, X.-P., & Xue, Y.-J. 2002a, *ApJ*, 569, 112
- Wu, X.-P., & Xue, Y.-J. 2002b, *ApJ*, 572, L19
- Wu, X.-P., Xue, Y.-J., & Fang, L.-Z. 1999, *ApJ*, 524, 22
- Zhang, P.-J., & Pen, U.-L. 2002, *ApJ*, in press (astro-ph/0202136)
- Zhang, P.-J., Pen, U.-L., & Wang, B. 2002, *ApJ*, in press (astro-ph/0201375)

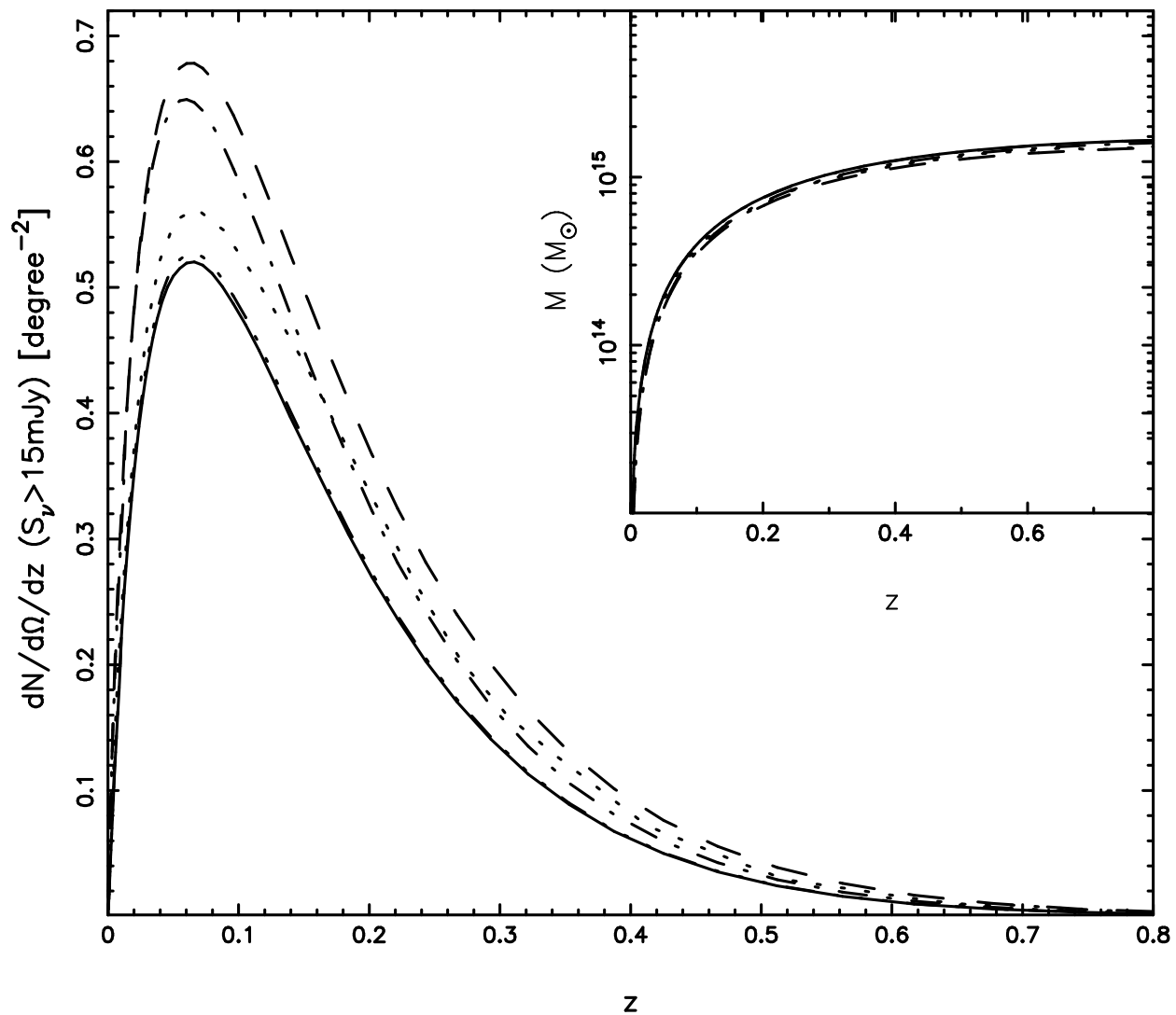


Fig. 1.— Expected redshift distribution of SZ cluster counts with $S_v = 15 \text{ mJy}$ at frequency 30 GHz. The results for five models with and without radiative cooling and under different assumptions of the intracluster gas in Table 1 are shown. Also illustrated in the inset is the minimum mass threshold against cluster redshift.

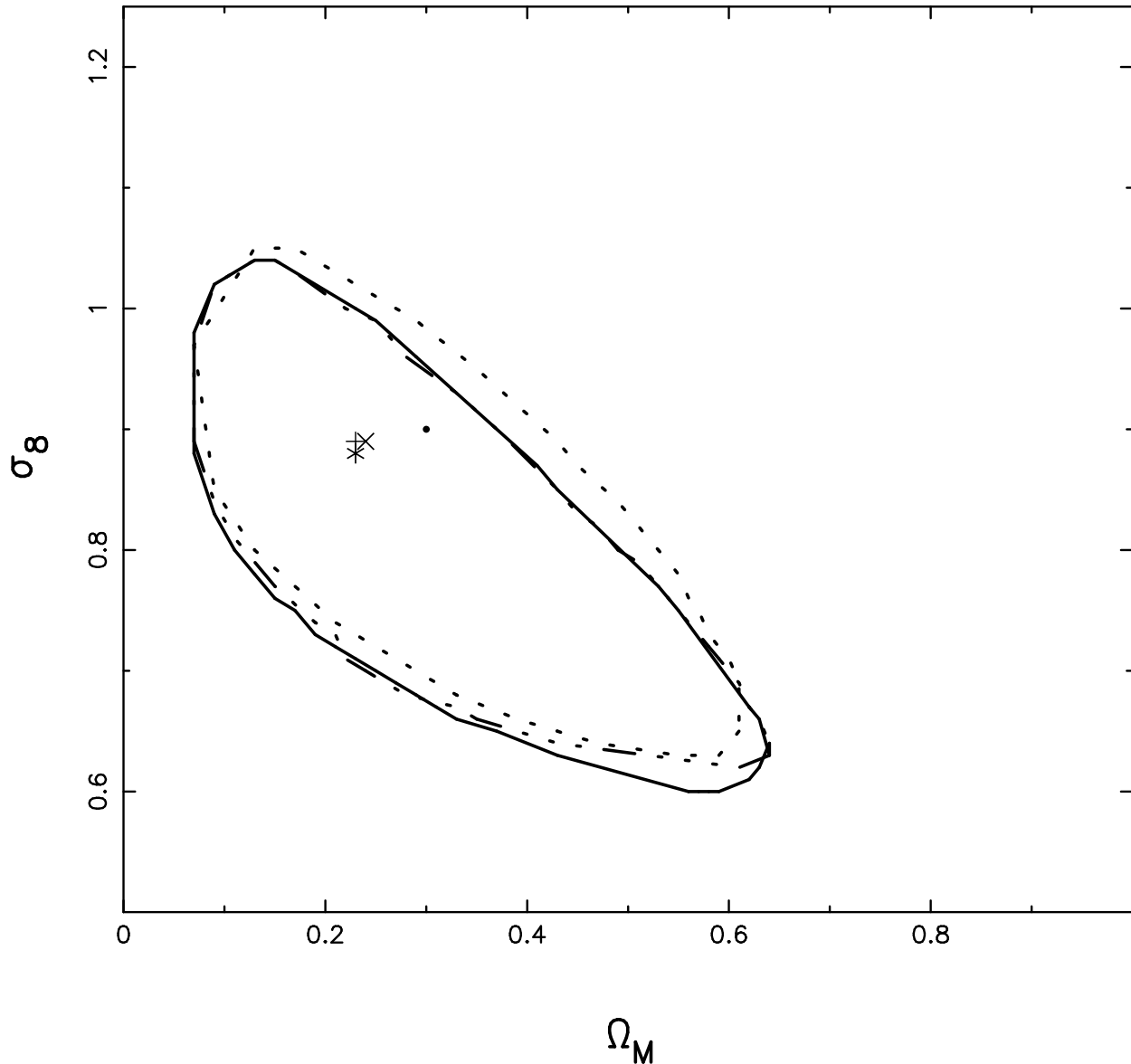


Fig. 2.— 68% joint confidence contours for Ω_M and σ_8 obtained by minimizing the χ^2 quantity: The redshift distribution of SZ cluster counts predicted by standard model (II) is required to match those by cooling models (see Table 1 for legend). A flat cosmological model of $\Omega_M + \Omega_\Lambda = 1$ is assumed. For the cooling models we have adopted $(\Omega_M, \sigma_8) = (0.30, 0.90)$ (indicated by the filled circle). The cross, asterisk and plus symbols represent the best-fit results for Model III, IV and V, respectively.

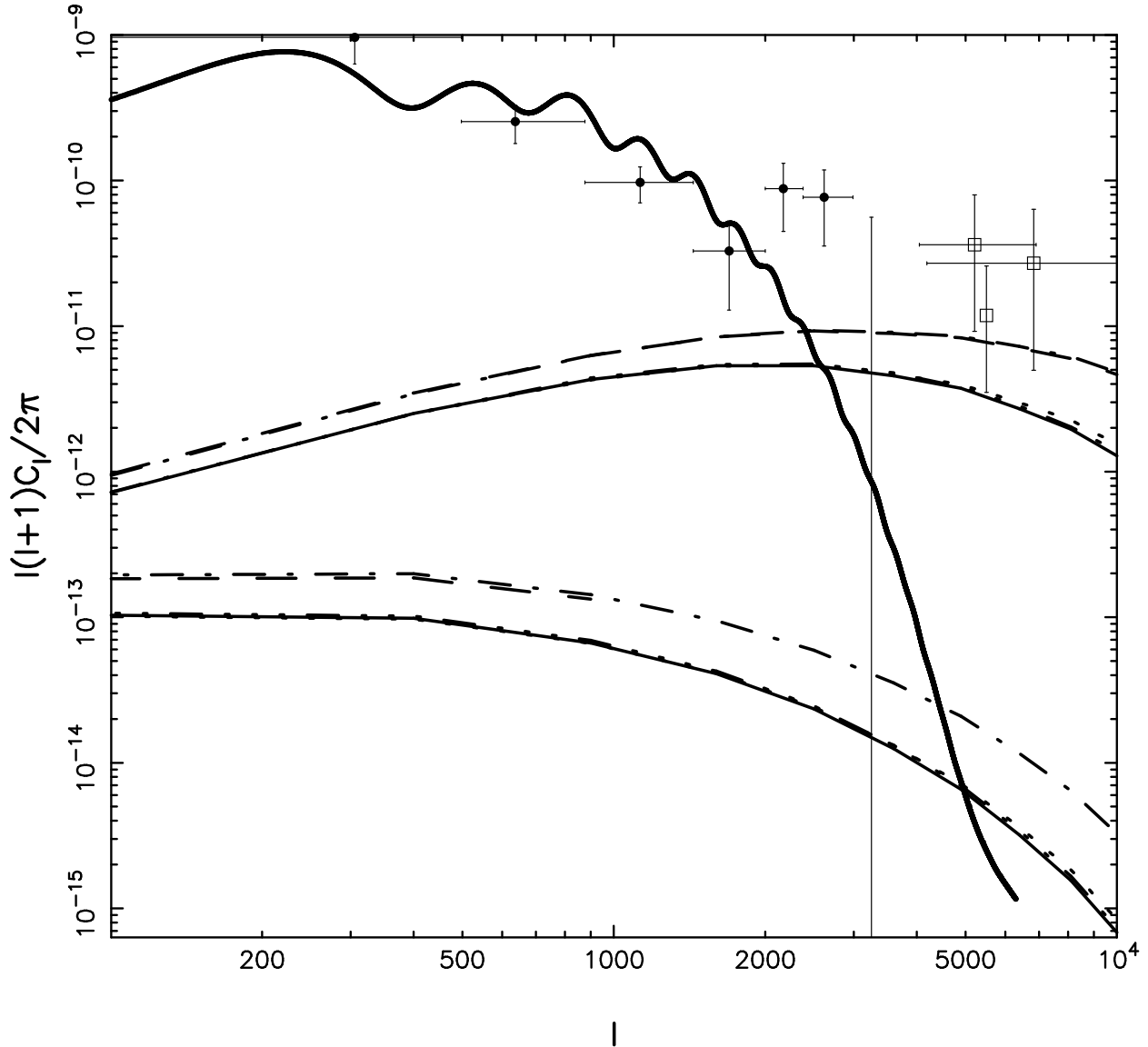


Fig. 3.— SZ power spectra from intracluster gas with and without radiative cooling (see Table 1 for legend). Top and bottom curves show the Poisson and clustering contributions, respectively. The upper thick solid line is the primary CMB signal predicted by CMBFAST. Recent observational results from BIMA (open squares; Dawson et al. 2001) and CBI (filled circles; Mason et al. 2002) are also shown.